FLUIDIZED BED DRYING OF SOYBEAN MEAL: THE EFFECT OF HYDRODYNAMICS USING COMPUTATIONAL FLUID DYNAMICS

Alexandre M. S. Costa, amscosta@uem.br
Danilo R. Rossi,
Paulo R. Paraíso,
Luiz Mário M. Jorge,
Fernanda Silva,
Universidade Estadual de Maringá Av. Colombo 5790, bloco 104 EMEC, Maringá, PR, 87020-900

Abstract. *In this work we investigate numerically the drying of soybean meal in a fluidized bed. Our modelling is implemented using the open-source code MFIX. For the code, the gas and solid phases are treated as inter-penetrating continua in an Eulerian framework Then, the locally-averaged (continuum) mass, momentum and energy balance, are solved using a modified version of the SIMPLE method. Here, we explore the effect of different parameters from hidrodynamics on the drying results: drag relationship between the two phases, method of solution for the solids granular energy, solids stress models, gas-phase turbulence, collisional and frictional coefficients. Towards validation of our modelling, the results are compared with a set of drying data for soybean meal from our experimental rig. The degree of accordance points to the better hidrodynamic model to be used.*

Keywords*: fluidized bed, drying, computational fluid dynamics, MFIX*

1. INTRODUCTION

The fundamental goal during soybean meal production is a quality product with a minimum cost. The drying process contributes to final moisture approaches to the desired levels. Fluidized bed drying involves simultaneous heat, mass and momentum transfer process, giving a highly non-linear set of governing equations. Also numerous parameters affect drying processes, many of them material dependent. The process has a long record of theoretical models whose predictions have been wildly different from actual results, and equipment that has failed to meet its design specification. Industrial design manufacturers have tended to rely on empirical scale-up rules based on pilot-plant testing, rather than published theoretical models. The very limited acceptance of academic theories for drying by industrial users has also been due to bad experiences when attempts were made to use published theory for practical design (Mujumdar, 2006). In spirit of their large application, understanding of the complex multi-phase flows involved in fluidized beds using computer simulations can became a good approach to the design, optimization, and control of industrial-scale fluidized bed driers. Availability of more sophisticated computer models is expected to result in greatly increased performance and reduced costs associated with fluidized bed driers implementation and operation. In this work is explored the effect of different parameters from hidrodynamics on the drying results predicted by a CFD code for a laboratory gas fluidized bed dryer.

2. EXPERIMENTAL SETUP

The experimental work was conducted at the Chemical Engineering Department of the Maringá State University. As shown in Fig. 1 the fluidized bed is composed of a cylindrical acrylic tube of 8.87 cm i.d. and 70 cm height. The air distributor is made of porous ceramic disc. A tap below the distributor is used to measure the air entering properties (temperature and relative humidity) by a digital psychrometer THWD-1 Amprobe Instruments. The pressure drop is measured by two pressure taps located right above the distributor and at the bed end. The air flow rate is controlled by three rotameters in parallel arrangement. The air is supplied by an industrial compressor and flow through an electrical resistance bank for heating.

The minimum fluidization velocity (u_{mf}) was 71 cm/s and was determined by the curve pressure drop versus air velocity according to procedure outlined in Foust (1980). The drying experiments were performed for a gas superficial velocity of 139 cm/s and for three different entering air temperatures : 25, 39 and 50 C. The mass of soybean meal used was 200 g corresponding to a 5 cm bed height. The initial moisture X_0 was 0.1993 g liquid water/g of moist soybean meal. The last value was obtained measuring the mass difference after drying the samples in a oven at 105 C for a 24 h period.

The soybean meal granulometric analysis was performed with sieves of 5, 6, 8, 12, 20 and 150 mesh. Approaching the industrial conditions, the soybean mean particles greater than 5 mesh size and smaller than 150 mesh size were disposed. Following the analysis, the calculated Sauter mean diameter was 0.1 cm. The density and packed bed voidage were determined simultaneously by adding a known mass of soybean meal in a beaker filled with a known volume of water. The displaced water volume corresponds to the volume of the particles, then the density is calculated by the

quotient between mass and displaced volume. On the other hand, the quotient between volume of particles and volume of the bed gives the packed bed voidage of 0.346.

The experimental procedure is described next. Initially the flow rate was adjusted for the gas flowing through the empty tube. Next the gas inlet temperature was adjusted by controlling the dissipated power by the resistance bank. After that, the particulate is introduced by the top, beginning the data collection. The relative humidity of the exiting air were taken every 10 s and the inlet temperature and humidity was taken in the beginning and the end of each run.

The solid moisture $X_{s\text{-liquid-water}}$ in the bed for a given time t was obtained by using the exit air relative humidity UR data and a mass balance for the bed according to Eq. (1), where Q_0 is the air flow rate, ρ_{air} is the air density, P is the total pressure and P_{sat} is the gaseous water saturation pressure at exit temperature.

$$X_{s-liquid-water}(t) = X_0 - Q_0 \int_0^t \rho_{air} \frac{0.622\ \mathrm{UR}\ P_{sat}}{P - \mathrm{UR}\ P_{sat}} dt \tag{1}$$

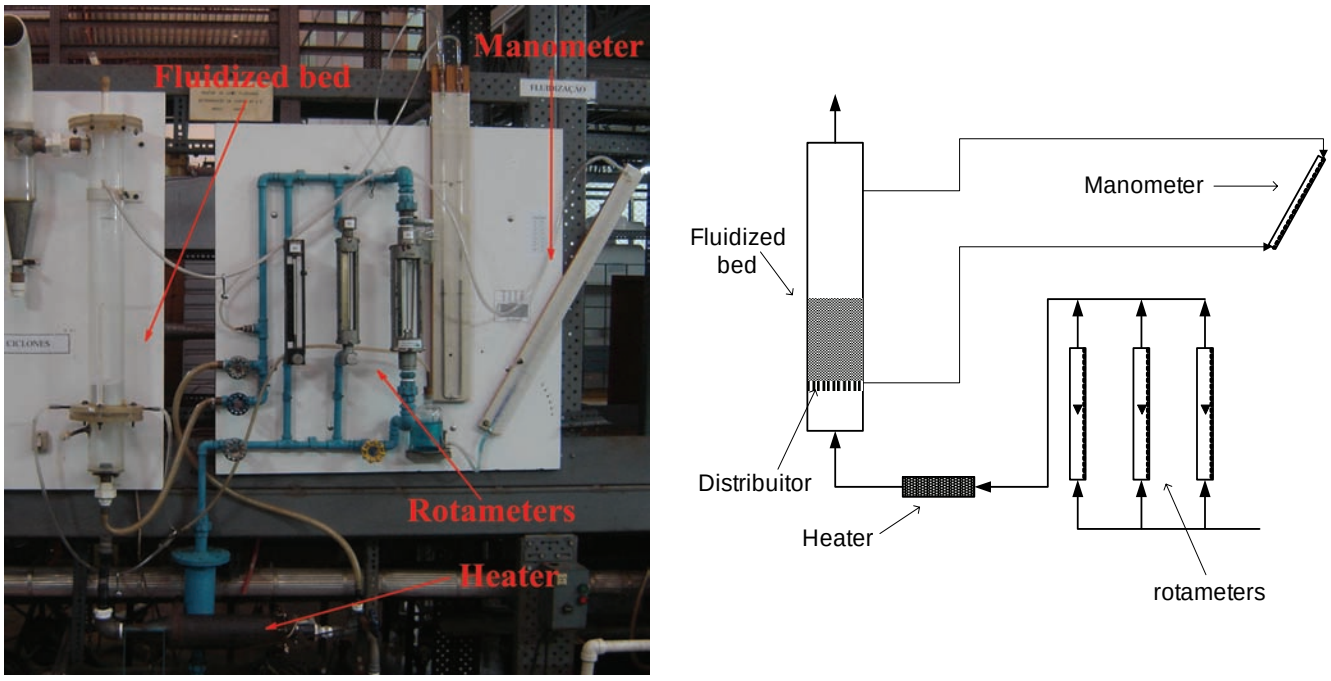

Figure 1. Experimental apparatus

3. MATHEMATICAL MODEL

The mathematical model is based on the assumption that the phases can be mathematically described as interpenetrating continua; the point variables are averaged over a region that is large compared with the particle spacing but much smaller than the flow domain (see Anderson, 1967). A short summary of the equations solved by the numerical code in this study are presented next. Refer to Benyahia et al. (2006) and Syamlal et al. (1993) for more detailment.

The continuity equations for the fluid and solid phase are given by :

$$\frac{\partial}{\partial t}\left(\varepsilon_f \rho_f\right) + \nabla \cdot \left(\varepsilon_f \rho_f \vec{v}_f\right) = \sum_{n=1}^{N_f} R_{fn} \tag{2}$$

$$\frac{\partial}{\partial t}\left(\varepsilon_s \rho_s\right) + \nabla \cdot \left(\varepsilon_s \rho_s \vec{v}_s\right) = \sum_{n=1}^{N_s} R_{sn} \tag{3}$$

In the previous equations ε_f, ε_s, ρ_f, ρ_s, $\vec{v}_f$ and $\vec{v}_s$ are the volumetric fraction, density and velocity field for the fluid and solids phases. The right side term in the continuity equations accounts for interphase mass transfer because of chemical reactions or physical processes, such as evaporation. The subscript n corresponds to the n chemical specie.

The momentum equations for the fluid and solid phases are given by:

$$\frac{\partial}{\partial t}\left(\varepsilon_f \rho_f \vec{v}_f\right) + \nabla\bullet\left(\varepsilon_f \rho_f \vec{v}_f \vec{v}_f\right) = \nabla\bullet\bar{\bar{S}}_f + \varepsilon_f \rho_f \vec{g} - \vec{I}_{fs} \tag{4}$$

$$\frac{\partial}{\partial t}\left(\varepsilon_s \rho_s \vec{v}_s\right) + \nabla\bullet\left(\varepsilon_s \rho_s \vec{v}_s \vec{v}_s\right) = \nabla\bullet\bar{\bar{S}}_s + \varepsilon_s \rho_s \vec{g} + \vec{I}_{fs} \tag{5}$$

$\bar{\bar{S}}_f$ $\bar{\bar{S}}_s$ are the stress tensors for the fluid and solid phase. It is assumed newtonian behavior for the fluid and solid phases. Moreover, the solid phase behavior is divided between a plastic regime (also named as slow shearing frictional regime) and a viscous regime (also named as rapidly shearing regime). The constitutive relations for the plastic regime are related to the soil mechanics theory On the other hand, the viscous regime behavior is ruled by kinetic theory related parameters.

$\vec{I}_{fs}$ is the momentum interaction term between the solid and fluid phases. In his formulation there is a term proportional to velocities differences between phases: the drag coefficient β. There is a number of correlation the drag coefficient. The first of the correlations for the drag coefficient is based on Wen and Yu (1966) work. The Gidaspow drag coefficient is a combination between the Wen Yu correlation and the correlation from Ergun (1952). The correlation proposed by Syamlal and O'Brien (1993) carries the advantage of being adjustable for different minimum fluidization conditions. The drag correlation from Hill, Koch and Ladd (2001) work is based on Lattice-Boltzmann simulations. The blended drag correlation originally proposed by Lathowers and Bellan (2000) allows controlling the transition from the Wen and Yu, and Ergun based correlations.

Equation (5) is a transport equation for the granular energy Θ. Its solution provides a way of determine the pressure and viscosity for the solid phase during the viscous regime. The terms κ_s γ and ϕ_{gs} are the granular energy conductivity, dissipation and production, respectively.

$$\frac{3}{2}\left[\frac{\partial}{\partial t}\varepsilon_s \rho_s \Theta + \nabla\bullet\rho_s \vec{v}_s \Theta\right] = \bar{\bar{S}}_s : \nabla\vec{v}_s - \nabla\bullet\left(\kappa_s \nabla\Theta\right) - \gamma + \phi_{gs} \tag{6}$$

The energy equations in terms of temperatures T_f and T_s for the fluid and solid phases are given in Eqs. (7) and (8). The specific heat and conductive flux for the fluid and solid phase are denoted by C_{pf}, C_{ps}, $\vec{q}_f$ and $\vec{q}_s$, respectively. The second term in the right hand side of Eqs. (7) and (8) accounts for the thermal energy transfer between the phases. The last terms in Eqs (7) and (8) accounts for the enthalpy variation due to chemical or phase change reactions. For the energy equation the following assumptions were made : no viscous dissipation, no pressure work, no radiation exchange effects.

$$\varepsilon_f \rho_f C_{pf}\left[\frac{\partial T_f}{\partial t} + \left(\vec{v}_f \bullet \nabla\right) T_f\right] = -\nabla\bullet\vec{q}_f + \gamma_{fs}\left(T_s - T_f\right) - \Delta H_f \tag{7}$$

$$\varepsilon_s \rho_s C_{ps}\left[\frac{\partial T_s}{\partial t} + \left(\vec{v}_s \bullet \nabla\right) T_s\right] = -\nabla\bullet\vec{q}_s - \gamma_{fs}\left(T_s - T_f\right) - \Delta H_s \tag{8}$$

The species transport equations in terms of mass fractions X_{fn} and X_{sn} for the chemical species in the fluid and solid phases are given by Eqs. (9) and (10): In these equations the diffusive effects were neglected. The terms R_{fn} and R_{sn} represents the fluid and solids species production due to a chemical or phase change reaction. For our case of study, we considered the solid phase containing two species : liquid water and dry soybean meal. The fluid phase is considered composed of two species : gaseous water and dry air. The phase reaction is modeled according to Eq. (11), where C is an adjustable constant, and the superscript eq corresponds to the saturation values.

$$\frac{\partial}{\partial t}\left(\varepsilon_f \rho_f X_{fn}\right) + \nabla\bullet\left(\varepsilon_f \rho_f \vec{v}_f X_{fn}\right) = R_{fn} \tag{9}$$

$$\frac{\partial}{\partial t}\left(\varepsilon_s \rho_s X_{sn}\right) + \nabla\bullet\left(\varepsilon_s \rho_s \vec{v}_s X_{sn}\right) = R_{sn} \tag{10}$$

$$R_{s-liquid-water} = C\left(X^{eq}_{g\text{-gaseous-water}} - X_{g\text{-gaseous-water}}\right) \tag{11}$$

4. NUMERICAL METHOD

MFIX (Multiphase Flow with Interphase eXchanges) is an open source CFD code developed at the National Energy Technology Laboratory (NETL) for describing the hydrodynamics, heat transfer and chemical reactions in fluid-solids systems. It has been used for describing bubbling and circulating fluidized beds, spouted beds and gasifiers. MFIX calculations give transient data on the three-dimensional distribution of pressure, velocity, temperature, and species mass fractions.

The hydrodynamic model is solved using the finite volume approach with discretization on a staggered grid. A second order accurate discretization scheme was used and superbee scheme was adopted for discretization of the convective fluxes at cell faces for all equations in this work. With the governing equations discretized, a sequential iterative solver is used to calculate the field variables at each time step. The main numerical algorithm is an extension of SIMPLE. Modifications to this algorithm in MFIX include a partial elimination algorithm to reduce the strong coupling between the two phases due to the interphase transfer terms. Also, MFIX makes use of a solids volume fraction correction step instead of a solids pressure correction step which is thought to assist convergence in loosely packed regions. Finally, an adaptive time step is used to minimize computation time. See Syamlal (1998) for more details.

For generating the numerical results and comparison with our experimental results we employed the parameters given in Table 2

Table 2. Input parameters for CFD

DT = 10^{-4} s	D_{bed} = 4,435 cm
LEQ_IT = 200	ε_{mf} = 0,346
LEQ_TOL = 10^{-8}	μ_f = 1.8 10^{-4} g/cm s
MAX_NIT = 50	ρ_f = 1.2 10^{-3} g/cm^3
DEF_COR = .TRUE.	d_p = 0.1 cm
NORM_G = 0.0	ρ_s =1.24 g/cm^3
NORM_S = 0.0	e = 0.8
t_{stop} = 10 s	$\phi = 30^o$

In this work, the remaining parameters for controlling the numerical solution (e.g., under-relaxation, sweep direction, linear equation solvers, residual tolerances) were left as their default values.

Figure 2 shows the initial and boundary conditions for the numerical simulations. The numerical runs were based on an axisymmetrical cylindrical coordinate system. The grid employed after mesh refinement studies was 20 (radial) × 80 (axial).

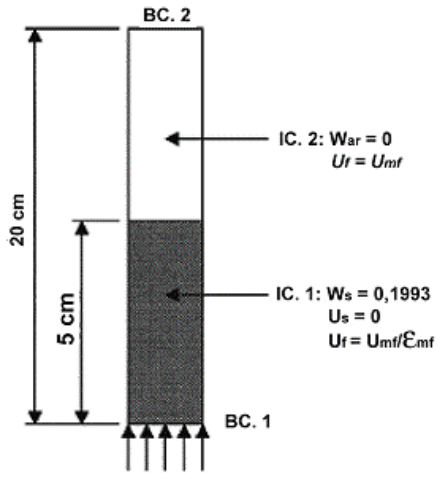

Figure 2. Initial conditions (IC) and boundary condition (BC) for CFD simulations.

5. RESULTS AND DISCUSSION

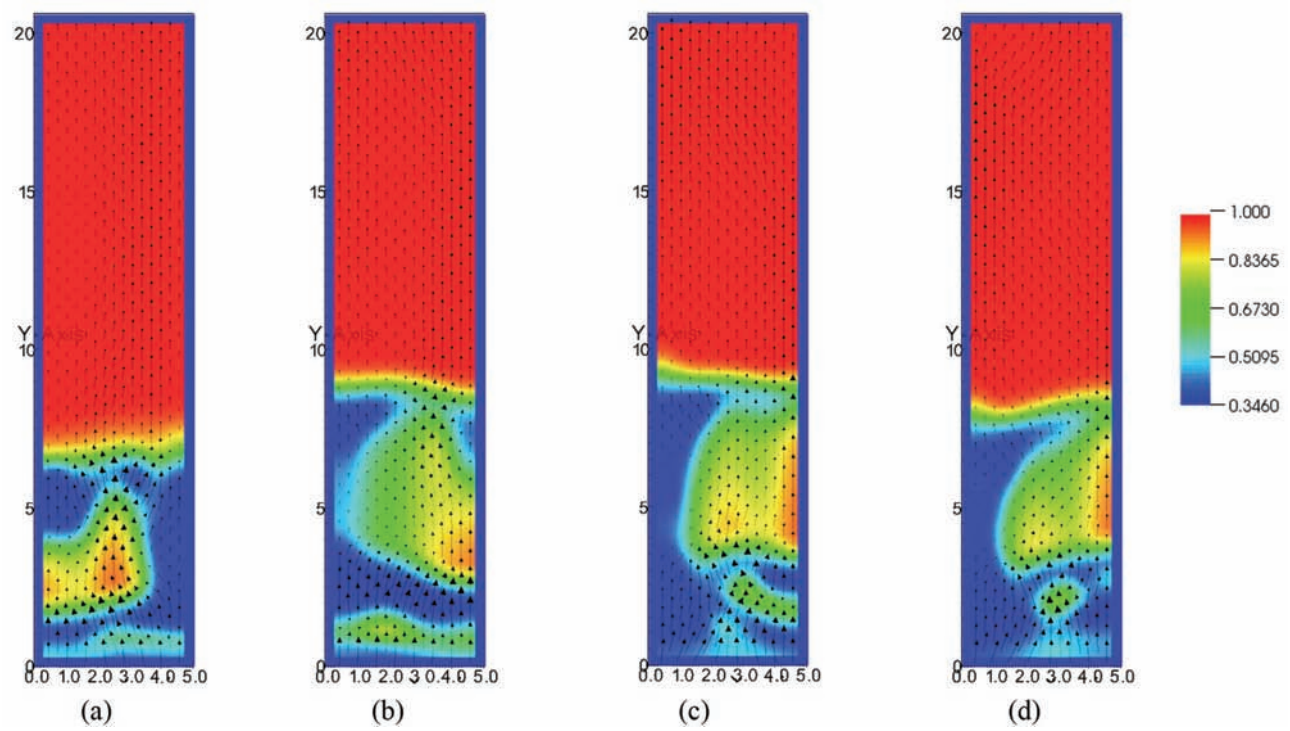

Figure 3. Instantaneous velocity and voidage fields. (a) 20.0 s, (b) 20.2 s, (c) 20.4 s, (d) 20.6 s

Figure 3 is a sampling plot showing the instantaneous gas velocities and gas volumetric fraction fields for different times. It clearly shows the high voidage regions (bubbles) in the dense bed .

The effect of changes on the hydrodinamic model on the final drying results are presented next. All the results for drying will be given in terms of an averaged liquid water mass fraction for the dense part of the fluidized bed. Figure 4 shows the effect of abolishing the slow shearing frictional regime. As can be seen from Fig. 4, disregarding the frictional regime implies in a slower rate of drying when compared with the use of the frictional regime.

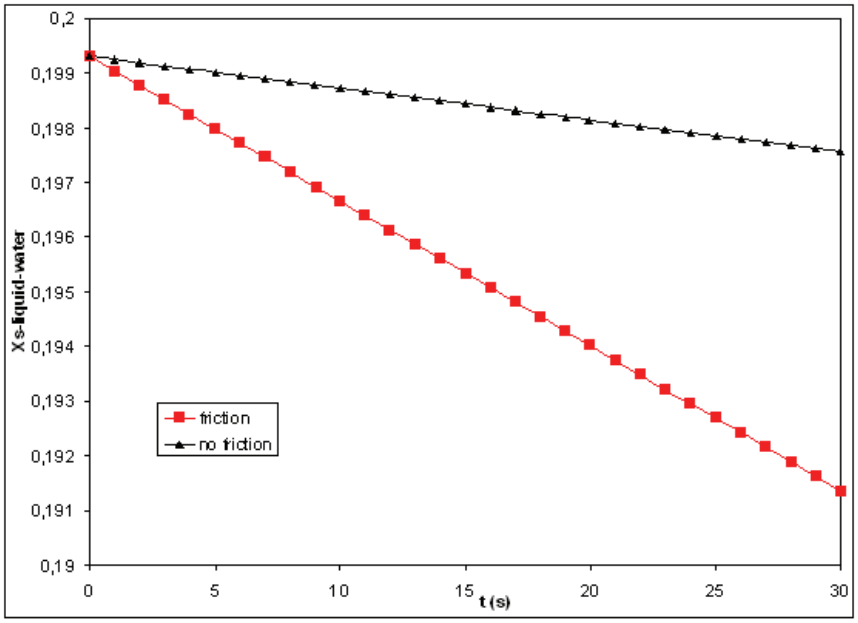

Figure 4. Effect of friction models on the drying results (no friction, friction).

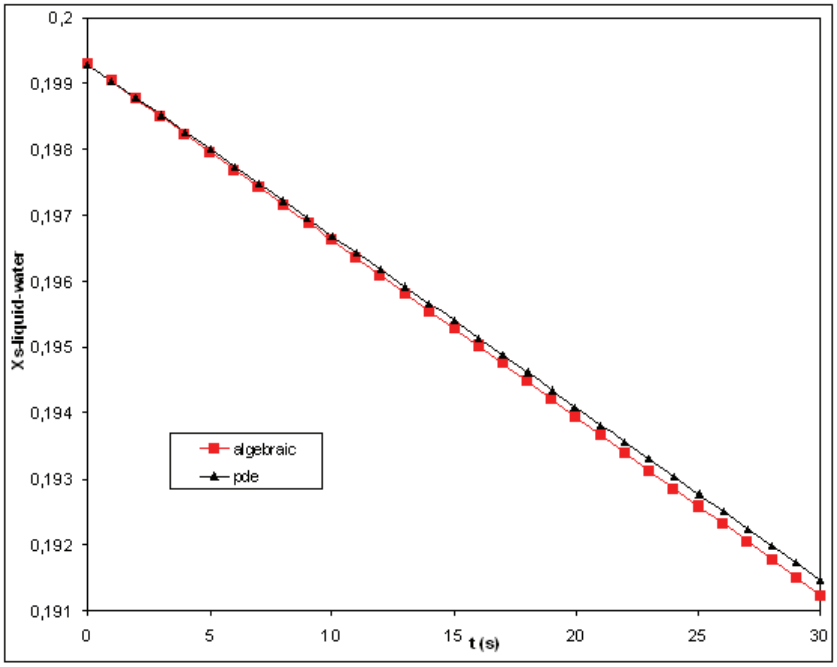

Figure 5. Effect of algebraic versus pde on the drying results (pde, algebraic).

Figure 5 shows the effect of considering just two terms of granular temperature equation, the first and the third term in the right side of Eq. (5). This approach is called algebraic approach and is less computationally expensive than solving the full partial diferential equation (pde) given in Eq. (5). As can be seen from figure there is no considerable effect in the results for using the algebraic approach

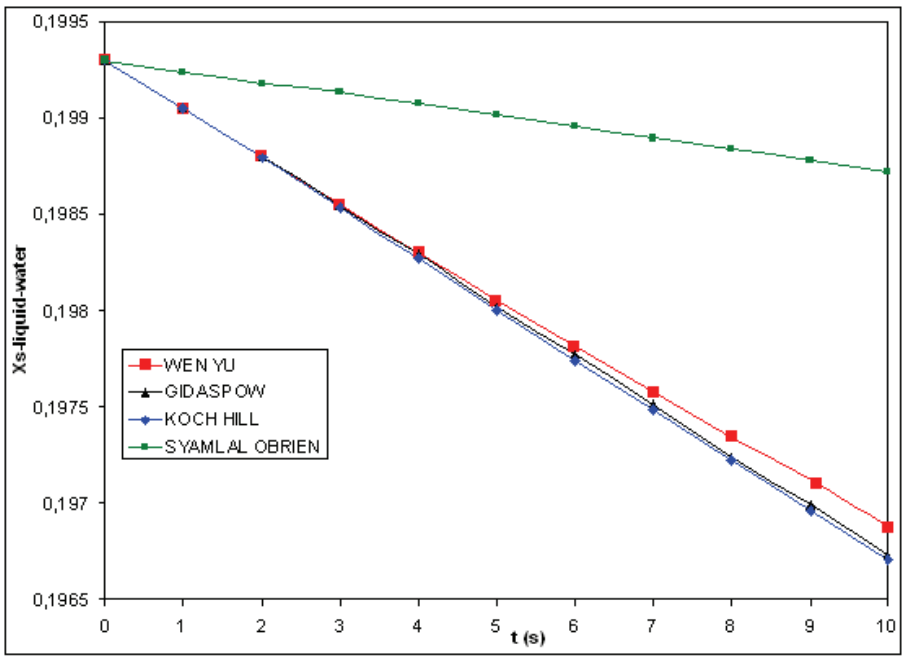

Figure 6. Effect of different drag correlations on the drying results.

Figure 6 shows the effect of using different correlations for the drag term. Except Syamlal and Obrien drag correlation all the remaining drag correlations predicted the same degree of water content decaying for the soybean meal. As Syamlal and Obrien drag correlation is the only that can be adjusted for the experimental minimum fluidization velocity, their results were used for comparison with experimental data.

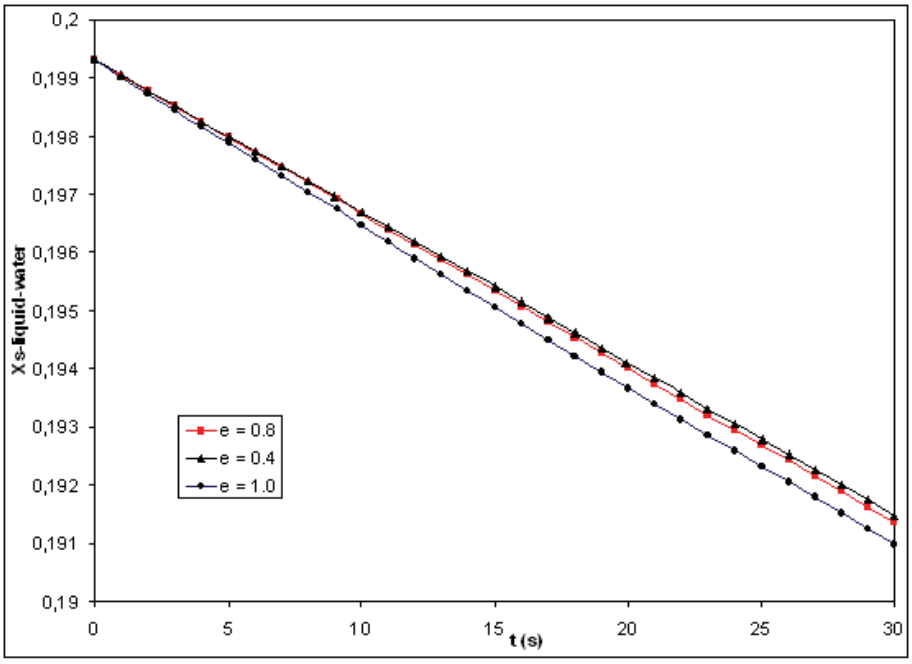

Figure 7. Effect of restitution coefficient.

Figure 7 shows the effect of the restitution coefficient on the predicted drying results. The restitution coefficient e is a parameter used in the kinetic theory model for the solids viscosity and pressure. When e decreases from 1 to zero the collisions spans from perfectly elastic to inelastic. The fig. 7 shows that the perfectly elastic collision predicts a more intense degree of decaying in the water content for the soybean meal. As perfectly elastic collision is not realistic approach for modeling the particles in the fluidized bed, we employed e = 0.8 for comparison with the experimental data.

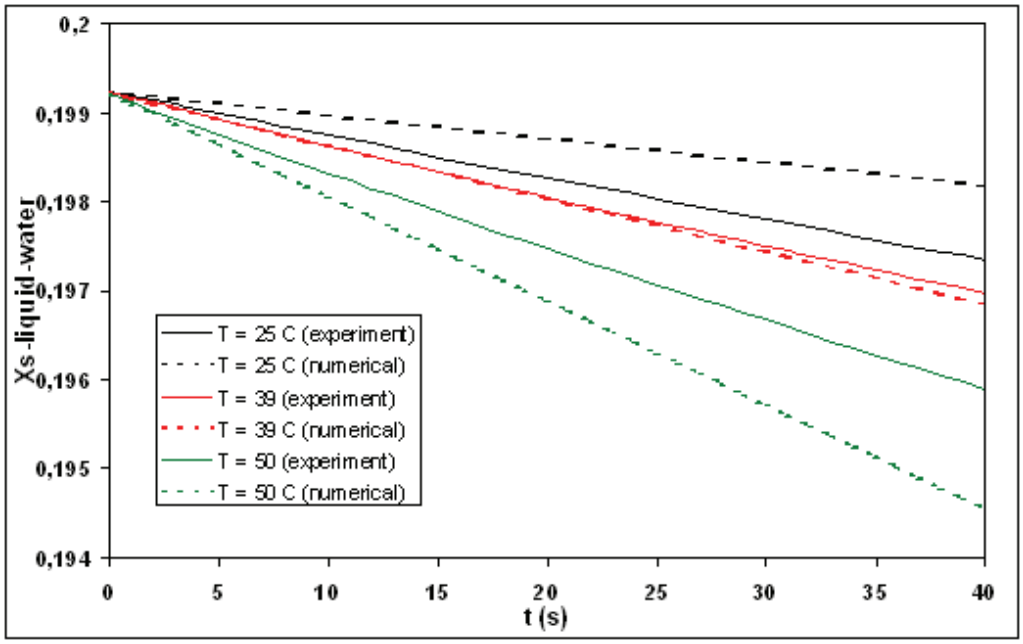

Figure 8. Comparison with experimental data for different air temperature entering values and U_f=139cm/s.

Figure 8 shows the numerical and experimental values for 3 different air entering values and for a fixed superficial velocity U_f. The best agreement was obtained for the intermediate temperature (T = 39 C). For the lower temperature (T = 25 C) the numerical results overpredicted the drying rate, whereas for the highest temperature the drying rate was underpredicted. These results points to the adjustment of the phase change rate coefficient C given in Eq. 10 according to the entering temperature

6. CONCLUSIONS

The available mathematical model and numerical code can be used to predict the hydrodynamics and drying kinetics for drying of soybean meal in a fluidized bed. In this work the results points to sensitivity of the results for parameters of the bed hidrodynamics. The results are very sensitive to neglecting the frictional regime. On the other hand the algebraic approach for calculating the granular energy can be used without prejudice. The effect of using different drag correlations are more noticeable for.the Syamlal Obrien drag correlation. The effect of the restitution coefficient is more noticeable for inelastic collisions. Finally, comparison with experimental data available from our experimental rig points toward better validation and show the potentials for use of CFD in fluidized bed drying.

7. ACKNOWLEDGEMENTS

The support from MFIX users forum and CENAPAD-SP is gratefully acknowledged

8. REFERENCES

Anderson, T. B., 1967, “A fluid mechanical description of fluidized beds: Equations of motion”, Industrial Engineering Chemical Fundamentals, Vol 6, pp. 527-539.

Benyahia, S., Syamlal, M., O’Brien, T. J., “Summary of MFIX Equations 2005-4”, 1 March 2006: <http://www.mfix.org/documentation/MfixEquations2005-4-1.pdf>.

Ergun, S., 1952, “Fluid-flow through packed columns”, Chemical Engineering Progress, Vol 48, n. 2, pp. 91-94.

Foust, A. S., 1980, “Principles of Unit Operations”, Wiley, N. York, USA, 768 p.

Hill, R. J., Koch, D. L., Ladd, J. C., 2001, “Moderate-Reynolds-number flows in ordered and random arrays of spheres”, Journal of Fluid Mechanics, Vol 448, p. 243-278.

Hill, R. J., Koch, D. L., Ladd, J. C., 2001, “The first effects of fluid inertia on flows in ordered and random arrays of spheres”, Journal of Fluid Mechanics, Vol 448, pp. 213-241.

Lathowers, D., Bellan, J., 2000, “Modeling of dense gas-solid reactive mixtures applied to biomass pyrolysis in a fluidized bed”, Proceedings of the 2000 U.S. DOE Hydrogen Program Review, NREL/CP-570-28890. USA.

Mujumdar, A. S., 2006, “Handbook of Industrial Drying”, CRC, N. York, USA, 1312 p.

Syamlal, M., 1998, “MFIX Documentation, Numerical Techniques”, Technical Note, DOE/MC-31346-5824, NTIS/DE98002029, National Technical Information Service, Springfield, VA, USA.

Syamlal, M., Rogers, W. A., O’Brien, T. J., 1993, “MFIX Documentation, Theory Guide”, Technical Note, DOE/METC-94/1004, NTIS/DE94000087, National Technical Information Service, Springfield, VA, USA.

Wen, C. Y., Yu, Y. H., 1966, “Mechanics of Fluidization”, Chemical Engineering Progress Symposium Series, Vol 62, n. 62, pp. 100-111.

5. RESPONSIBILITY NOTICE

The authors are the only responsible for the printed material included in this paper.